Int. J. Heat Mass Transfer. Vol. 35, No. 7, pp. 1753–1761, 1992
Printed in Great Britain

0017–9310/92 $5.00+0.00

Analysis of bubble translation during transient flash evaporation

SRIDHAR GOPALAKRISHNA
IBM Corporation, Endicott, NY 13760, U.S.A.

and

NOAM LIOR
Department of Mechanical Engineering and Applied Mechanics,
University of Pennsylvania, Philadelphia, PA 19104, U.S.A.

(*Received* 13 *June* 1990 *and in final form* 18 *June* 1991)

Abstract—An analysis was performed of the rise characteristics of bubbles, which are also growing, in a pressure field which is decreasing exponentially with time. The bubble rise and growth occur due to flash evaporation caused by reducing the pressure in the vapor space above a pool of liquid. Basset's bubble momentum equation was modified to include the effects of the generated pressure wave, and to include bubble growth. The solution of the differential equation was obtained for three different expressions for the bubble drag, for pressure ratios of 0.1–0.9, Jakob numbers of 5–113, Weber numbers of 0–0.16, and time constants of the pressure transient down to 5 ms. Results indicate that different bubble drag expressions give bubble velocities which differ by as much as 100%. The pressure term introduced by the authors has a negligible effect in the range of parameters considered here but becomes significant for very rapid depressurization rates, and the initial velocity of the bubble has little effect on the bubble's subsequent rise velocity.

1. INTRODUCTION

FLASH evaporation occurs when the vapor pressure above a liquid is reduced to a level which is below the saturation pressure corresponding to the temperature of the liquid. Typically, most of the vapor is liberated through bubbles released from the liquid after a process of nucleation, growth and rise to the liquid–vapor interface. Typically, the pressure reduction process is transient, where often the initial pressure drop is large and it decays in time to a new state of equilibrium. Such a process is common to many applications in which flash evaporation plays an important role, such as distillation, vacuum freezing, and loss of coolant accidents (LOCA) in nuclear power plants. The primary objective of this study is to examine bubble translation accompanied by growth inside a liquid which is exposed to a pressure field decaying with time.

Motion of bubbles and liquid droplets in fluids has been studied extensively in the past (cf. ref. [1]). Good results were obtained, particularly for the limiting cases of potential flow and for the steady-state terminal velocity. A vast amount of literature exists on the growth of bubbles. A number of researchers have studied the problem of combined rise and growth of bubbles, which is the objective of this study, but with the restricting assumptions of heat transfer controlled growth with rise induced purely by buoyancy (cf. refs. [2–4]). The present analysis removes these two restrictions by: (1) considering the entire regime of bubble growth, including the initial inertia-controlled growth period, by using the results of Mikić *et al.* [5]; and (2) by directly incorporating the effects of the transient pressure reduction term which drives the flash evaporation. The analysis is thus more general and covers bubble rise and growth not only in steady-state boiling but also in the transient process of flash evaporation.

2. PROBLEM FORMULATION

This section describes the problem formulation for the force balance on a vapor bubble which grows due to an imposed transient pressure reduction in the vapor space, and translates upward due to buoyancy and this pressure reduction. A force balance over a horizontal cross-section of the bubble is used in this study to determine the rise velocity for a given growth rate.

The major assumptions used in deriving the governing equation are:

1. The bubble nucleus already exists when flashing is initiated, most likely on a present micro-bubble (cf. ref. [6]).
2. The bubble is spherical.
3. The bubble rises vertically in a fluid of infinite expanse.
4. Growth is governed by the Mikić, Rohsenow and Griffith (MRG) [5] solution which accounts for the

NOMENCLATURE

C_D	drag coefficient
C_p	specific heat of the liquid
d_e	effective diameter of the bubble
g	gravitational acceleration
h_{fg}	latent heat of vaporization
Ja	Jakob number, $\Delta T C_p/h_{fg}$
k	thermal conductivity of liquid
Mo'	Morton number, $g\mu^4/\rho\sigma^3$
p_f	final pressure in the vapor space
p_i	initial vapor space pressure
p^*	pressure ratio, p_f/p_i
Pe	Peclet number, $2U_\infty R_0/\alpha_l$
R	bubble radius at any time t
R^+	dimensionless bubble radius in MRG expression
R_0	initial radius of the bubble
Re	Reynolds number, $2RU_\infty/\nu_l$
t	time
t_d	traversal time for the pressure wave
t^+	dimensionless time in MRG expression
T_0	initial temperature of the pool
T_{sat}	saturation temperature inside the bubble
T_∞	liquid temperature far away from the bubble
U_∞	liquid velocity far from the bubble
We	Weber number, $2RU_\infty^2\rho_l/\sigma$
x, y	spatial coordinates.

Greek symbols

α	thermal diffusivity
β	time constant of the depressurization
ΔT	superheat in the liquid
μ	viscosity
ξ_2	horizontal cross-section radius of the bubble
ρ	density
σ	surface tension.

successive inertial and thermal regimes during the bubble growth process.

5. The liquid is incompressible.

6. The pressure in the vapor space is an exponentially decaying function of time with a known, arbitrary, time constant.

7. The effect of non-condensable gases in the liquid is negligible.

The equation of motion for a growing bubble was written as a force balance over its cross-section. A schematic of the bubble translation in the vertical direction is shown in Fig. 1. This force balance can be derived from the basic equations of fluid mechanics starting with the Navier–Stokes equations (as developed for bubbles in non-flashing liquids by Basset [7]). Since the translation process examined here is transient, the net force was equated to the rate of change of vapor and liquid momentum. The resulting equation for the translation velocity, U_∞, in this flashing case, followed by a brief explanation of the terms, was written as:

$$\frac{d}{dt}\left(\tfrac{4}{3}\pi R^3\rho_v U_\infty + \tfrac{2}{3}\pi R^3\rho_l U_\infty\right) = \tfrac{4}{3}\pi R^3 g(\rho_l-\rho_v) + \frac{dp}{dt}t_d\pi R^2 - C_D\tfrac{1}{2}\rho_l U_\infty^2\pi R^2 - 4R^2\sqrt{(\pi\rho_l\mu_l)}\int_0^t \frac{dU_\infty}{dt}(t_1)\frac{1}{\sqrt{(t-t_1)}}\,dt_1. \quad (1)$$

The first term represents vapor inertia, and the second term on the left-hand side is the contribution of the added mass due to liquid displacement. The first term on the right-hand side is the buoyancy force, and the second term is the effect of the pressure wave traveling down from the vapor space due to the imposed pressure reduction. The modeling of this pressure term was carried out using an approximation for the complex interactions occurring during the pressure wave travel, a description of which is provided later in this section. The third term on the right-hand side is the drag force contribution which arises due to the frictional stresses. The drag coefficient used in this study is different from the conventionally used expression for drag because the change in bubble size with time is taken into account in the modeling. The last term represents a cumulative effect of past acceleration of the bubble weighted by the time elapsed, and is referred to in the literature as the 'Basset history term'. This term arises due to the dissipation of vorticity generated at the bubble surface into the liquid. It represents a higher order effect of the transient, and is usually neglected in practical situations. However, as pointed out in this paper, large depressurizations found in flash evaporation could lead to acceleration levels that make the contribution of the history term comparable to the other terms. An evaluation of its magnitude is carried out in the Appendix.

The driving forces are those of buoyancy and the applied pressure reduction, which tend to propel the bubble upward, the restraining forces being those of liquid inertia, added mass due to displacement of the liquid, unsteady drag force, and the Basset history term (which accounts for the prior acceleration history of the bubble).

Since $\rho_l/\rho_v \approx 1000$ for the flashing of water for typical temperatures and pressures, the contribution of vapor momentum on the left-hand side of equation (1) is negligible in comparison to the liquid momentum. Neglecting the vapor momentum and the history term

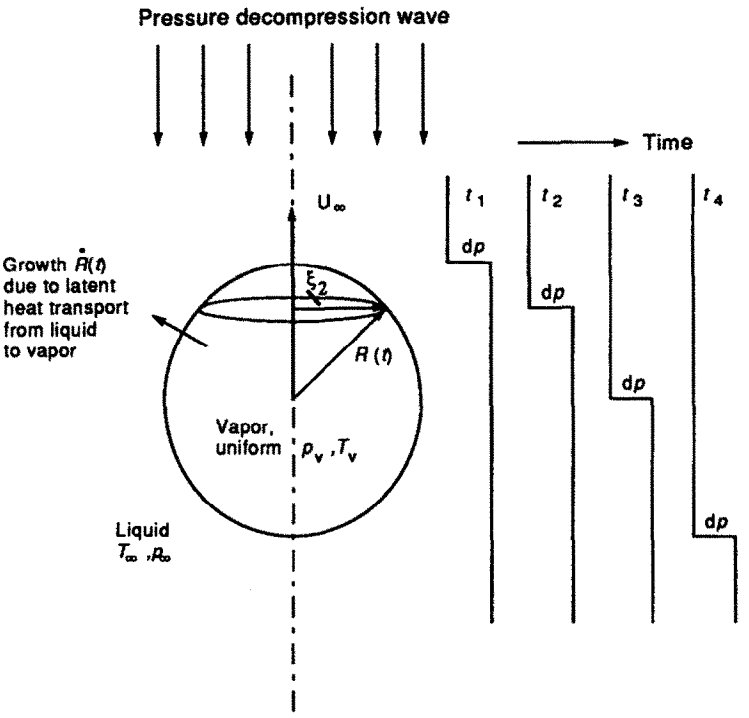

FIG. 1. Schematic of bubble translation and pressure wave propagation.

(such an assumption is plausible for the case of small pressure reductions encountered in flashing—which in turn leads to a small contribution to the integral in equation (1); this assumption is justified a posteriori using the calculated rise velocity—see the Appendix), equation (1) becomes

$$\frac{dU_\infty}{dt}+\frac{3U_\infty}{R}\frac{dR}{dt}-2g\frac{\rho_l-\rho_v}{\rho_l}-\frac{3}{2}\frac{dp}{dt}t_d\frac{1}{\rho_l R}+\frac{3}{4}C_D\frac{U_\infty^2}{R}=0. \quad (2)$$

Next, models for the growth, drag and pressure terms were inserted into the above equation to obtain a single equation for the rise velocity as a function of time.

We used the Mikić *et al.* [5] expression for the growth history of the bubble. This equation is valid for both inertial (initial) and thermally controlled (later) growth regimes, and is therefore well suited for the early stages of the growth process. For the conditions considered here, R/R_0 typically reaches a maximum of 50

$$R^+=\tfrac{2}{3}[(t^++1)^{3/2}-(t^+)^{3/2}-1] \quad (3)$$

where

$$R^+=\frac{AR}{B^2},\quad t^+=\frac{A^2t}{B^2}$$

$$A=\left[\frac{2}{3}\frac{\Delta Th_{fg}\rho_v}{T_{sat}\rho_l}\right]^{1/2}\quad B=\left[\frac{12}{\pi}Ja^2\alpha_l\right]^{1/2}$$

$$\text{and}\quad Ja=\frac{\rho_l}{\rho_v}\frac{c_p\Delta T}{h_{fg}}.$$

In this bubble translation analysis, the unsteady nature of the drag coefficient was modeled using a quasi-steady approximation. Drag expressions which have been derived in the literature for constant size bubbles are used here, but the radius, and hence, the drag coefficient, is considered variable in the computations. A variety of expressions for the appropriate drag coefficient were tried out. One of the expressions is taken from the list compiled by Clift *et al.* [1] (shown in Table 1) for the range of translation Reynolds number Re $(=2RU_\infty/\nu_l)$ corresponding to this investigation. It was found that the translation process is quite sensitive to the value of the drag coefficient, and widely differing results can be obtained by using different available methods for its determination. A list of the drag expressions used in this study is shown in Table 1.

The drag coefficient is also affected by the Morton number. Miyahara and Takahashi [8] have found that the drag coefficient for bubbles is constant for Reynolds numbers (based on equivalent diameter) larger than 10. They also found a 0.3 power dependence of C_D on the Morton number for small Reynolds numbers, i.e.

Table 1. Drag coefficients for spherical bubbles

• Moore [15] (fluid spheres)

$$C_D = \frac{48}{Re}\left[1 - \frac{2.21}{\sqrt{(Re)}} + O(Re^{5/6})\right] \quad (4)$$

• Peebles and Garber terminal velocity expression [13] (rigid spheres)

$$C_D = \frac{8}{3}\frac{R^2}{1.82}\frac{\rho_l g}{\sigma} \quad (R \geq 0.07\ \text{cm}) \quad (5)$$

• Fluid sphere drag [1]

Re	C_D
0.1	191.8
1	18.3
5	4.69
10	2.64
20	1.40
30	1.07
40	0.83
50	0.723
100	0.405
200	0.266
300	0.204
400	0.165
500	0.125

$$C'_D = 0.03(Re')^{1.5}(Mo')^{0.3}$$

where

$$C'_D = C_D\left(\frac{d}{a}\right)^2, \quad Re' = \frac{Re}{d/a}, \quad Mo' = \frac{g\mu^4}{\rho\sigma^3},$$

and a = major axis diameter of the ellipsoidal bubble. They observed a change in the behavior of C_D with Re at a value of $Mo' = 10^{-7}$. For our calculations, Mo' is always below 10^{-7} and thus the behavior of the drag coefficient with Re as shown in Table 1 is valid.

The pressure term in equation (1) represents the effect of a depressurization (expansion) wave traveling down the liquid from the vapor space as a consequence of the imposed pressure reduction. Observations have shown [9, 10] that bubbles are accelerated upward soon after the pressure reduction is imposed, but then their upward motion settles down to a relatively quiescent rise pattern as they approach the surface. Due to the large pressure reduction rates that are possible in situations where rapid depressurization is used, such a pressure drop could exert an impulse propelling the bubble upward. This effect on bubble rise complements that due to buoyancy.

The strength of this expansion wave depends on the depth at which bubble nucleation occurs (the depressurization effect is suppressed due to the hydrostatic pressure) and on the rate of depressurization. The duration of the effect is determined by the time of passage of the wave moving vertically across the bubble surface. The excess pressure which causes bubble motion in the upward direction (superimposed on the gravity field), acts over progressively increasing areas of cross-section until the wave reaches the bubble equator, then it acts over decreasing areas. As shown in Fig. 1, the pressure difference dp acts over the radius ξ_2, which is a function of bubble radius and time. The net contribution to the pressure impulse is $dp \times \pi\xi_2^2$, and an integral of this contribution over time represents the total pressure force. As can be seen from the functional form of the imposed pressure reduction, the contribution becomes progressively smaller, and the initial impulse is the largest contributing factor.

A limiting case of this entire phenomenon of the pressure wave travel—that of the total pressure drop acting over the maximum area of πR^2 for the period of time t_d it takes for the wave to travel across the bubble—was considered in this study.

The pressure reduction imposed externally in the vapor space was modeled as an exponential decay with time (cf. ref. [11])

$$p = p_f + (p_i - p_f)\,e^{-\beta t}. \quad (6)$$

The growth of this bubble is strongly affected by the pressure reduction, and this is accounted for by using the Jakob number (which is proportional to the imposed superheat) in the growth expression.

For the largest depressurization rates encountered in conditions of LOCA, with $\beta = 1000\ s^{-1}$, the pressure term is approximately 27 m s^{-2}, comparable in magnitude to the constant buoyancy term. However, the high contribution acts only for the duration of time that the pressure reduction wave takes to cross the bubble.

The equations for the drag coefficient, pressure reduction and growth were inserted into equation (2), and this results in a non-linear ordinary differential equation for the rise velocity U_z as a function of time:

$$\frac{dU_z}{dt} + \frac{9}{2}U_z\frac{A^2}{B^2}\left[\frac{(t^+ + 1)^{1/2} - t^{+1/2}}{(t^+ + 1)^{3/2} - t^{+3/2} - 1}\right] - \frac{2g\Delta\rho}{\rho_l} + \frac{81}{2}\frac{\mu_l}{\rho_l}U_z\frac{A^2}{B^4}[(t^+ + 1)^{3/2} - t^{+3/2} - 1]^{-2} + \frac{B^2}{A}[(t^+ + 1)^{3/2} - t^{+3/2} - 1](p_i - p_f)\beta\,e^{-\beta t_d}\frac{\pi t_d}{\rho_l} = 0 \quad (7)$$

where A and B were defined in equation (3), and equation (5) was used here for the drag coefficient.

The initial velocity for the integration of equation (7) was taken to be a finite, small non-zero number (typically 0.01 m s^{-1}). Since the magnitude of this initial bubble velocity depends on the circumstance of bubble nucleation and on the surrounding flow field at that time and place, various values of the initial velocity were examined to establish the dependence of the solution on the initial conditions.

To compare the results obtained from the above integration with oft-employed models which assume potential flow for the calculation of terminal rise velocity (cf. ref. [12]) for a given growth rate, the expression

Table 2. Range of parameters used in this study

Quantity	Minimum	Maximum
Pressure ratio, p^*	0.1	1.0
Jakob number, Ja	8.5	113
Weber number, We	0	0.16
Radius, R (mm)	0.5	5
Time constant, β^{-1} (ms)	5	∞
β (s^{-1})	0	200

$$U_{\text{potential}} = \frac{2q}{R^3}\int_0^t R^3\,\mathrm{d}t \qquad (8)$$

was evaluated numerically for the radius growth curve given by the MRG expression. The range of parameters used in this study is shown in Table 2.

3. SOLUTION PROCEDURE

Equation (7) was integrated numerically starting from $t = 0^+$ using a locally fifth-order Runge–Kutta scheme. The integration was carried out for various pressure reductions in the vapor space, as characterized by the values of p^* and β in the expression

$$p - p_f = (p_i - p_f)\,e^{-\beta t} = p_i(1-p^*)\,e^{-\beta t}. \qquad (9)$$

Here, $(p_i - p_f)$ represents the overall imposed pressure drop.

The integration is carried out until the combination of the velocity U_∞ and the bubble radius R result in a Weber number which is greater than the limit specified for the sphericity condition to be valid ($We \approx 0.16$). Beyond this time limit, the bubble shape (spheroidal or ellipsoidal) will influence the rise velocity, and needs to be determined simultaneously.

During the integration, care was taken to maintain a time step compatible with the assumption of a pressure wave impacting on the bubble surface. In other words, the time step used in the calculations must be of the same order as the time spent by the wave in traversing the bubble surface, so that the process can be modeled with sufficient accuracy. A time step of 1 μs was used in all the computations, so that the estimated wave travel time ($\approx 7.8 \times 10^{-7}$ s) can be followed closely in most of the cases of interest. As the bubble radius increases, this time step describes the phenomenon sufficiently well.

In addition to computation of the bubble velocity, the magnitude of each of the terms contributing to the momentum equation was also examined.

4. RESULTS AND DISCUSSION

Figure 2 shows the rise velocity as a function of time for different levels of superheat imposed on the liquid, and for three different expressions for the drag coefficient (C_D). As shown in Fig. 2, the results depend strongly on the drag coefficient expression employed.

The potential flow solution (equation (6)), generated for comparison with limiting cases, shows that the translation velocity increases linearly with time. The usage of C_D from Peebles and Garber [13] results in the rise velocity going through a maximum, as shown in Fig. 2. The maximal rise velocity decreases as the overall pressure reduction increases (corresponding to lower p^*), because the drag as well as the growth terms impede the motion and therefore cause deceleration of the bubble (see equation (7) for the sign of each of the terms). For small overall pressure drops ($p^* = 0.9$), the curve is almost coincidental with the potential flow curve for the rise of a bubble in water. As the imposed pressure drop increases, the growth term contributes more and more to the deceleration, leading to a maximum in the rise velocity.

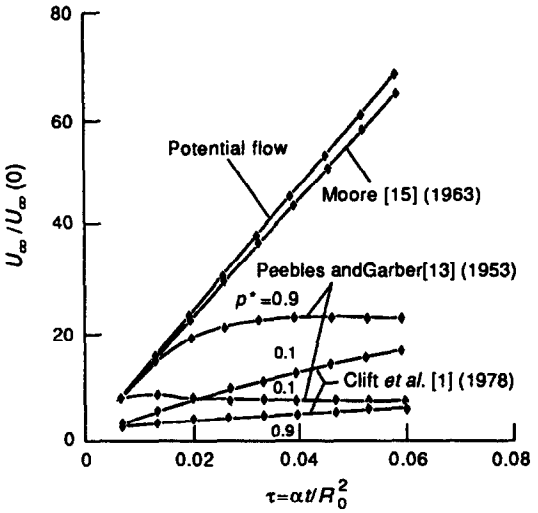

FIG. 2. Bubble rise velocity history for different rise velocities as a function of time for various expressions of the drag coefficients taken from Table 1, and for different pressure ratios; $\beta = 200\ s^{-1}$, $U_r(0) = 0.01\ m\ s^{-1}$.

The observed trend of lower velocity for higher p^* (or Jakob number) is confirmed by the results of Pinto and Davis [3], who obtained maximum rise velocities of 25 cm s^{-1} for a Jakob number of 5, whereas the maximum velocity reached only about 12 cm s^{-1} for $Ja = 50$ (Fig. 3). As also seen in the comparison of individual contributions to the acceleration (Fig. 4), the drag term exerts a large influence and, eventually, the velocity decreases as a function of time. Also seen in Fig. 2 is the fact that increasing pressure drops cause the velocity maximum to occur sooner.

The individual contributions of buoyancy, pressure reduction, drag and growth terms in the force balance equation (equation (7)) are examined further below for the various drag expressions used in the calculations. The five terms from equation (7) are labeled as Net Acceleration, Growth, Buoyancy, Drag, and Pressure, respectively, in Figs. 4 and 5, for $p^* = 0.9$

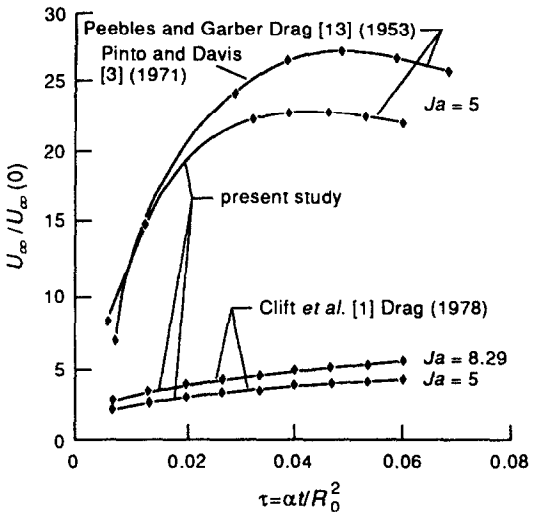

FIG. 3. Comparison of results with Pinto and Davis [3].

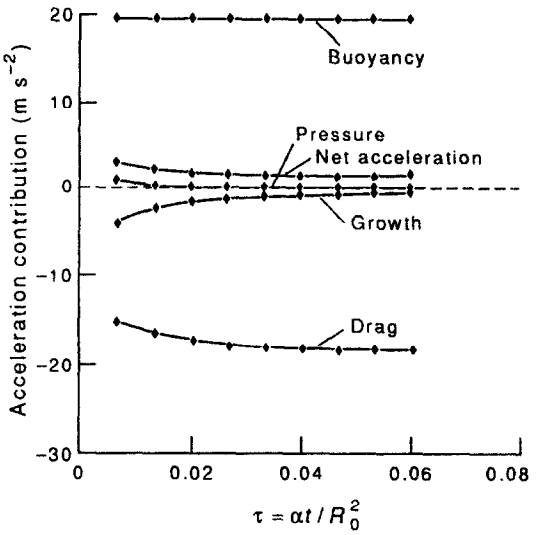

FIG. 5. Individual contributions to the force balance; $p^* = 0.9$, $\beta = 200\ s^{-1}$, $U_z(0) = 0.01\ m\ s^{-1}$. Drag coefficients based on Clift *et al.* [1], shown in Table 1.

and $\beta = 200\ s^{-1}$. These figures can be examined in conjunction with Fig. 2, which describes the rise velocity. When using the Peebles and Garber drag expression, the maximum velocity attained around $\tau = 0.025$ is seen to be the result of an exact balance between buoyancy on the one hand and growth and drag on the other. The growth term decreases from the initial high value to almost zero for large times, because of the decrease in growth rate. The gravity (or buoyancy) term remains practically constant for the conditions specified, with only minor changes caused by variations in vapor density. The graphs shown here are typical, and a similar trend is followed for other pressure reductions which have been examined in this study.

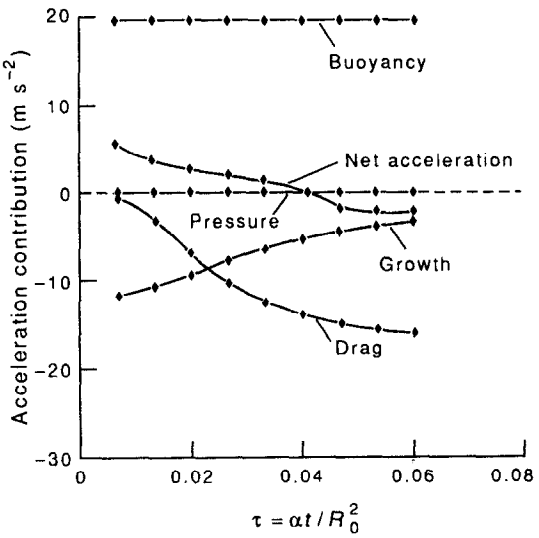

FIG. 4. Individual contributions to the force balance: $p^* = 0.9$, $\beta = 200\ s^{-1}$, $U_z(0) = 0.01\ m\ s^{-1}$, Peebles and Garber drag.

The pressure term was observed to be quite small, relatively negligible in the entire range of parameters p^* and β investigated here. Larger and faster depressurizations can occur in situations such as nuclear reactor loss of coolant accidents (cf. ref. [14]). Using the drag coefficient expression proposed by Moore [15], the pressure term corresponding to LOCA conditions ($\beta = 1000\ s^{-1}$) was found to be about 20% of the buoyancy term at the initial instant of time, not a negligible quantity.

The bubble velocity calculations based on drag coefficients developed for fluid spheres [1], summarized in Table 1, are also shown in Fig. 2 and are probably more representative of the actual situation because they are a function of the Reynolds number and were calculated more accurately using weighted residual methods and boundary layer theory for a range of Reynolds numbers. The trend shown is such that larger depressurizations now cause higher velocities of translation. An examination of the contribution of each term (Figs. 4 and 5) reveals the source of this behavior. The growth term obviously increases for the case of larger driving pressure reduction, and the influence of drag is felt at later times as a reduction in the slope of the curve. Since the coefficient of drag multiplies U_∞^2 / R in the force balance (equation (7)), a larger bubble size results in a smaller drag contribution to the overall deceleration of the bubble. This is in contrast to the Peebles and Garber [13] drag expression, which predicts an R^2 dependence of C_D. The drag expression from Clift *et al.* [1] predicts the lowest bubble rise velocities, and we believe that this is the most appropriate choice for

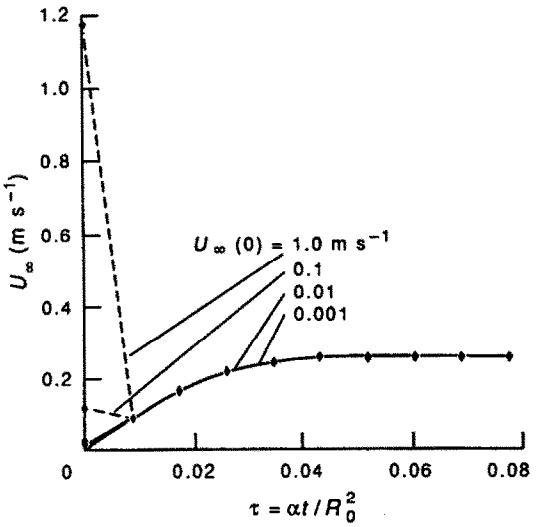

FIG. 6. Effect of initial velocity on bubble rise; Peebles and Garber drag, $p^* = 0.9$, $\beta = 200\ s^{-1}$.

the case of flash evaporation studied in this paper. In this connection, it should be mentioned that the expressions for drag used by Peebles and Garber [13] are for rigid spheres, whereas the other expressions are for fluid spheres. Surfactants are often present in the liquid and they accumulate on the surface of the bubble, which causes it to behave as a rigid sphere as far as fluid drag is concerned. During the early stages of formation and growth, the assumption of a fluid sphere is more appropriate, as demonstrated here.

This behavior was also confirmed by the use of another drag expression, developed from potential flow theory, by Moore [15]. As expected, the rise curve is linear, resembling the potential flow curve. For higher pressure reductions, the curve shifts upward, and due to zero skin friction drag, the bubble accelerates upward. There is no deceleration because the contribution of the growth term remains at a comparable level to that of buoyancy. Moore's expression obviously tends to overpredict the bubble rise velocity.

Figure 6 compares different initial velocity assumptions on the rise history for a given depressurization level. The effect of initial velocity is seen to be minimal, and a large initial value (such as 1 m s^{-1}) settles down rapidly to the predicted rise curve as shown. Such a situation arises because the drag term remains small, whereas the growth term is quite large initially. The net acceleration is a large, negative number because of its annihilation by the growth term alone. The drag term exerts an influence comparable to the others, as shown in Figs. 4 and 5. This shows that the driving forces are too great for the initial velocity to have an impact on the rise characteristics.

Varying the time constant of the depressurization (for $p^* = 0.9$), it was found that there is practically no difference in the rise pattern for three different rates corresponding to $\beta = 0$, $\beta = 20\ s^{-1}$, and $\beta = 200\ s^{-1}$. This is a direct consequence of the relatively small value of the pressure term in the present range of parameters, as discussed above.

5. CONCLUSIONS

1. The Basset equation was modified to include the effect of the pressure wave generated by depressurization on bubble rise velocity.

2. Using the Mikić, Rohsenow and Griffith equation for bubble growth [5], and a number of available expressions for drag coefficient for spheres, this modified Basset equation was solved to determine the transient bubble rise velocity during flash evaporation caused by transient depressurization.

3. The contributions of all the driving forces acting on the vapor bubble growing and translating in the time-varying pressure field were also examined, including the extent of influence of the pressure reduction force introduced in this study.

4. The effect of the imposed superheat is quite important in determining the rise velocity characteristics. An almost linear increase in velocity was obtained for a high overall pressure drop ($p^* = 0.1$). As the imposed pressure reduction was decreased ($p^* = 0.9$), the retardation sets in early, and only 20% of the velocity reached for $p^* = 0.1$ is reached in this case for the case of drag coefficients from Clift *et al.* [1].

5. The effect of the newly introduced pressure term is short-lived and practically insignificant in the range of parameters investigated here, contributing only about 0.1% for the case of flash evaporation at normal temperatures and pressure for the flashing of water, but becomes more significant as the magnitude and rate of depressurization increase.

6. The initial bubble rise velocity (post-nucleation) plays only a marginal role in the eventual rise process, because its effects are largely cancelled by the large influence of the growth and drag processes as soon as the bubble starts moving.

7. The nature of the drag expression in the unsteady case is very influential in determining the resulting rise velocity. Different drag expressions result in up to a 100% difference in rise velocity depending upon the range of application.

Acknowledgements—This work was supported in part by the U.S. Department of Energy through the Solar Energy Research Institute, and by a scholarship from the International Desalination Association to one of the authors (SG). Professor O. Miyatake from Kyushu University provided many valuable comments.

REFERENCES

1. R. Clift, J. R. Grace and M. E. Weber, *Bubbles, Drops and Particles*. Academic Press, New York (1978).
2. N. Tokuda, W. J. Yang and J. A. Clark, Dynamics of moving gas bubbles in injection cooling, *J. Heat Transfer* **90**, 371–378 (1968).

3. Y. Pinto and E. J. Davis, The motion of vapor bubbles growing in uniformly superheated liquids, *A.I.Ch.E. Jl* **17**, 1452–1458 (1971).
4. E. Ruckenstein and E. J. Davis, The effects of bubbles translation on vapor bubble growth in a superheated liquid, *Int. J. Heat Mass Transfer* **14**, 939–952 (1971).
5. B. B. Mikić, W. M. Rohsenow and P. Griffith, On bubble growth rates, *Int. J. Heat Mass Transfer* **13**, 657–666 (1970).
6. N. Lior and E. Nishiyama, The effect of gas bubbles on flash evaporation, *Desalination* **45**, 231–240 (1983).
7. A. B. Basset, *A Treatise on Hydrodynamics*, Vol. 2, pp. 285–302. Dover, New York (1961).
8. T. Miyahara and T. Takahashi, Drag coefficient of a single bubble rising through a quiescent liquid, *Int. Chem. Engng* **25**, 146 (1985).
9. O. Miyatake, K. Murakami, Y. Kawata and T. Fujii, Fundamental experiments with flash evaporation, *Heat Transfer Jap. Res.* **2**(4), 89–100 (1973).
10. R. J. Peterson, S. S. Grewal and M. M. El-Wakil, Investigations of liquid flashing and evaporation due to sudden depressurization, *Int. J. Heat Mass Transfer* **27**, 301–310 (1984).
11. S. P. Kung and T. W. Lester, Boiling transition during rapid decompression from elevated pressures, ASME Paper 81-WA/HT-57 (1981).
12. R. H. Cole, *Underwater Explosions*. Dover, New York (1959).
13. F. N. Peebles and H. J. Garber, Studies on the motion of gas bubbles in liquids, *Chem. Engng Prog.* **49**, 88 (1953).
14. J. H. Lienhard, M. Alamgir and M. Trela, Early response of hot water to sudden release from high pressure, *J. Heat Transfer* **100**, 473–479 (1978).
15. D. W. Moore, The boundary layer on a spherical gas bubble, *J. Fluid Mech.* **16**, 161–176 (1963).
16. M. S. Plesset and S. A. Zwick, The growth of vapor bubbles in superheated liquids, *J. Appl. Phys.* **25**, 493–500 (1954).

APPENDIX: EVALUATION OF THE ORDER OF MAGNITUDE OF THE BASSET HISTORY INTEGRAL

The Basset history term can be written as

$$F_H = 4R^2\sqrt{(\pi\rho_l\mu_l)}\int_0^t \frac{dU_\infty}{dt}(t_1)\frac{1}{\sqrt{(t-t_1)}}\,dt_1. \quad (A1)$$

Typically, $\rho_l = 1000$ K g m^{-3}, and $\mu_l = 10^{-3}$ N s m^{-2}. For the highest accelerations, obtained in potential flow [12]

$$U_\infty = \frac{2g}{R^3}\int_0^t R^3\,dt. \quad (A2)$$

For the growth defined by $R \propto t^{3/2}$, we get

$$U_\infty = \frac{2g}{K^3 t^{9/2}}K^3\frac{t^{11/2}}{11/2} = \frac{4gt}{11}. \quad (A3)$$

Therefore

$$\frac{dU_\infty}{dt}(t_1) = \frac{4g}{11} = 3.567 \text{ m s}^{-2}.$$

The history term now becomes

$$F_H = 4\times5\times10^{-3/2}\times\sqrt{(\pi\times1000\times10^{-3})}\int_0^t\frac{3.567}{\sqrt{(t-t_1)}}dt_1$$

$$= 1.265\times10^{-3}\sqrt{t} \text{ where } t \text{ is in seconds.}$$

For the times considered here, i.e. $t \approx 0.1$ s, the history term contributes approximately 0.0004 N.

In comparison to the above estimate for the history term, the typical contribution of the other terms is

Gravity

$$\tfrac{4}{3}\pi R^3 g(\rho_l-\rho_v) = 0.00514 \text{ N}.$$

This term is therefore at least one order of magnitude higher at the largest radius (and the highest acceleration) than the history term.

Drag

$$C_D\tfrac{1}{2}\rho_l U_\infty^2\pi R^2 = 0.00499 \text{ N}$$

(for $C_D = 1$: a high value, see Clift *et al.* [1], Table 1). For the present calculations, therefore, the effect of the history term can be safely neglected.

ANALYSE DE LA TRANSLATION DES BULLES PENDANT L'EVAPORATION BRUSQUE

Résumé—On analyse les caractéristiques de la montée des bulles, lesquelles grossissent, dans un champ de pression qui diminue exponentiellement dans le temps, ce qui modélise l'évaporation brusque par réduction de pression dans l'espace de vapeur au-dessus du liquide. L'équation du momentum de la bulle selon Basset est modifiée pour inclure les effets de l'onde de pression générée, ainsi que la croissance des bulles. La solution de l'équation est obtenue pour trois expressions différentes de la trainée de la bulle, pour des rapports de pression de 0,1 à 0,9, des nombres de Jakob de 5 à 113, des nombres de Weber de 0 à 0,16 et des constantes de temps allant jusqu'à 5 ms pour la pression. Les résultats indiquent que des expressions différentes de la trainée de bulle donnent des vitesses qui peuvent différer de 100%. Le terme de pression introduit par les auteurs a un effet négligeable dans le domaine des paramètres considéré ici mais il devient significatif pour les dépressurisations rapides; et la vitesse initiale de la bulle a un effet très faible sur la croissance ultérieure de la vitesse.

UNTERSUCHUNG DER BLASENBEWEGUNG BEI DER ENTSPANNUNGSVERDAMPFUNG

Zusammenfassung—Das Aufstiegsverhalten von wachsenden Dampfblasen in einem zeitlich exponentiell abfallenden Druckfeld wird untersucht. Blasenaufstieg und -wachstum werden durch Entspannungsverdampfung erzeugt, indem der Druck im Dampfraum über einer Flüssigkeit abgesenkt wird. Die Blasenimpulsgleichung nach Basset wird modifiziert, um den Effekt der durch die Druckabsenkung erzeugten Druckwelle einzubeziehen. Die Differentialgleichung wird für folgende Bedingungen gelöst: drei unterschiedliche Ausdrücke für den Strömungswiderstand der Blasen, Druckverhältnisse von 0,1 bis 0,9, Jakob-Zahlen von 5 bis 113, Weber-Zahlen von 0 bis 0,16 und Zeitkonstanten der Drucktransienten bis hinunter zu 5 ms. Die Ergebnisse zeigen, daß unterschiedliche Formulierungen für den Strömungswiderstand der Blasen Unterschiede in der Blasenaufstiegsgeschwindigkeit bis zu 100% verursachen. Der von den Autoren eingeführte Druckterm hat im untersuchten Wertebereich der verschiedenen Parameter einen vernachlässigbaren Einfluß, wird aber wichtig für sehr hohe Druckabsenkungsgeschwindigkeiten. Die Anfangsgeschwindigkeit der Blasen beeinflußt die sich später einstellende Aufstiegsgeschwindigkeit der Blasen wenig.

АНАЛИЗ ПОСТУПАТЕЛЬНОГО ДВИЖЕНИЯ ПУЗЫРЬКОВ В ПРОЦЕССЕ НЕУСТАНОВИВШЕГОСЯ ИСПАРЕНИЯ ПРИ ВСПЫШКЕ

Аннотация—Анализируются характеристики подъема растущих пузырьков в поле давлений, экспоненциально уменьшающемся со временем. Подъем и рост пузырьков происходят за счет испарения при вспышке, которое обусловлено уменьшением давления в объеме пара над жидкостью. Уравнение Бассе для количества движения пузырьков модифицируется с учетом эффектов формирующейся волны давления и роста пузырьков. Получено решение этого дифференциального уравнения при трех различных напряжениях для сопротивления пузырьков, отношениях давлений 0,1–0,9, числах Якоба 5–113, числах Вебера 0–0,16, а также постоянных времени, характеризующих падение давления, составляющих до 5 мс. Результаты показывают, что различные выражения для сопротивления пузырьков дают скорости пузырьков, отличающиеся на 100%. Эффект введенного авторами слагаемого, содержащего давление, пренебрежимо мал в исследуемом диапазоне изменения параметров, но становится существенным при очень быстром сбросе давления, в то время как начальная скорость пузырька слабо влияет на скорость его последующего подъема.